

Quantum interface between an electrical circuit and a single atom

D. Kielpinski,¹ D. Kafri,² M. J. Woolley,³ G. J. Milburn,⁴ and J. M. Taylor²

¹*Centre for Quantum Dynamics, Griffith University, Nathan, QLD 4111, Australia*

²*Joint Quantum Institute/NIST, College Park, MD, USA*

³*Centre for Engineered Quantum Systems, School of Mathematics and Physics, The University of Queensland, St Lucia, QLD 4072, Australia*

⁴*Centre for Engineered Quantum Systems, School of Mathematics and Physics, The University of Queensland, St Lucia, Australia 4072*

We show how to bridge the divide between atomic systems and electronic devices by engineering a coupling between the motion of a single ion and the quantized electric field of a resonant circuit. Our method can be used to couple the internal state of an ion to the quantized circuit with the same speed as the internal-state coupling between two ions. All the well-known quantum information protocols linking ion internal and motional states can be converted to protocols between circuit photons and ion internal states. Our results enable quantum interfaces between solid state qubits, atomic qubits, and light, and lay the groundwork for a direct quantum connection between electrical and atomic metrology standards.

Atomic systems are remarkably well suited to storage and processing of quantum information [1, 2]. However, their properties are tightly constrained by nature, causing difficulties in interfacing to other optical or electronic devices. On the other hand, quantum electronic circuits, such as superconducting interference devices, may be easily engineered to the designer's specifications and are readily integrated with existing microelectronics [3]. The naturally existing couplings between a single atom and a single microwave photon in a superconducting circuit are too weak for practical coherent interfaces. The coupling has been estimated at tens of Hz [4], much smaller than the decoherence rate of 10^3 s^{-1} . For trapped ions, the coupling between the electric dipole induced by ion motion and the electric field of the superconducting circuit can be much larger, on the order of several hundred kHz. Unfortunately, this coupling is far off resonance. Motional frequencies of trapped ions are limited to tens of MHz, while any superconducting circuit must maintain GHz operating frequencies to avoid thermal noise, even in the extreme cryogenic environment of a dilution refrigerator.

In this Letter, we propose a method to couple single trapped ions with microwave circuits, bridging the gap between the very different frequencies of ion motion and microwave photon by parametric modulation of the microwave frequency. The resulting coupling strength of $\sim 2\pi \times 60 \text{ kHz}$ is sufficient for high-fidelity coherent operations and similar to the strength of currently obtained ion-ion couplings [5, 6]. A simple model system illustrating the key concepts is shown in Fig. 1. Microwave photons reside in a superconducting LC circuit with natural frequency $\omega_{\text{LC}} = 1/\sqrt{LC} \approx 1 \text{ GHz}$. A single ion is confined within the capacitor C_s and can oscillate at the motional frequency $\omega_i \approx 10 \text{ MHz}$. The circuit voltage across C_s generates an electric field that couples to the ion's motional electric dipole. Modulating the circuit capacitance by C_{mod} at a frequency ν causes the

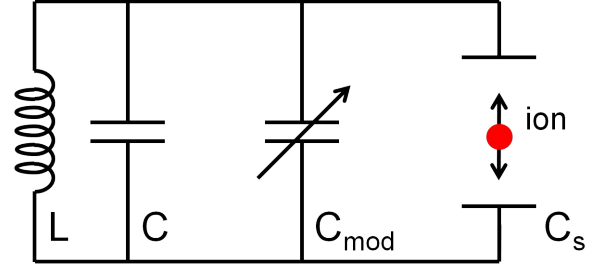


FIG. 1. Equivalent-circuit model of our scheme for ion-circuit coupling.

superconducting voltage to acquire sidebands at frequencies $\omega_{\text{LC}} \pm \nu$. The coupling between the superconducting circuit and the ion motion becomes resonant when $\omega_i \approx \omega_{\text{LC}} - \nu$. The interaction Hamiltonian is then

$$H_{\text{int}} = \hbar g a b^\dagger + \text{h.c.} \quad (1)$$

where a and b are the annihilation operators of the microwave photon mode and the ion motional mode, respectively. As shown below, $g \sim 2\pi \times 60 \text{ kHz}$.

The coupling between the LC circuit and the ion motion allows us to generalize all the well-known protocols operating on ion spin and motion to protocols operating on ion spin and LC state. Ion spin-motion protocols based on laser [7] or microwave fields [8, 9] now allow for generation of nearly arbitrary spin/motion entangled states. If the capacitance modulation is switched on for a time $T = \pi/(2g)$, Eq. (1) shows that the mode operators evolve as $a(T) = -ib(0)$, $b(T) = -ia(0)$, i.e., a perfect swap between LC and motional modes. For a unitary operator $U(b, \vec{\sigma})$ describing a protocol between the ion motion and the ion spin operator $\vec{\sigma}$, the sequence 1) swap LC/motion, 2) apply $U(b, \vec{\sigma})$, 3) swap LC/motion implements the same unitary $U(a, \vec{\sigma})$ between the LC and spin modes. By this means, one can establish a quantum communications channel between LC circuits

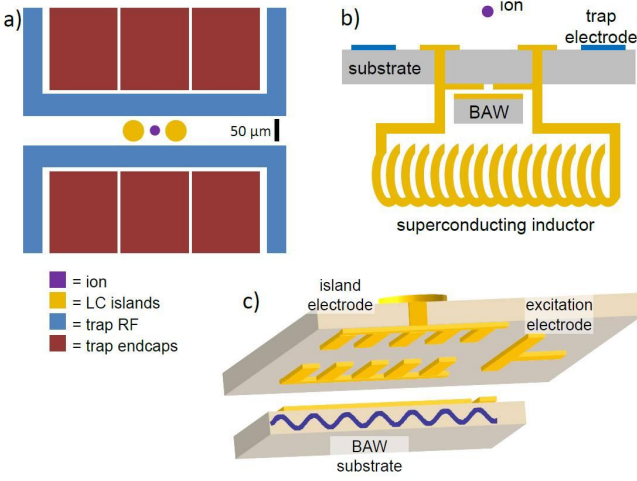


FIG. 2. Schematic of a device for coupling trapped ions to a microwave resonant circuit. a) Top view of surface ion trap showing RF and DC trapping electrodes. The “LC island” electrodes couple the ion motion to the LC circuit excitation. b) Side view of device, showing ion trap, superconducting inductor, and BAW device. c) Exploded side view of BAW device. Purple line: transverse displacement of BAW substrate due to classical driving.

in separate dewars, couple ion spins through a common LC circuit for large-scale quantum computing on a single chip, and perform Heisenberg-limited voltage metrology in the microwave domain by generating large Schrödinger cat states of the LC mode.

Realisation of ion-CQED coupling.— Figure 2 shows a schematic of a device implementing the simple model described above. The device combines an ion trap, a microwave LC circuit, and a bulk-acoustic-wave (BAW) microelectromechanical modulator to coherently couple the quantized motion of trapped ions at MHz frequencies with microwave photons at 1 GHz. We now describe a specific design to give real-world parameters relevant to our system.

Ions are confined above a planar electrode structure of a type now widely used for microfabricated trap arrays [10]. Applying appropriate voltages to the electrodes generates RF electric fields, which provide a ponderomotive confining potential transverse to the trap axis, and DC fields that give rise to a harmonic potential along the axis. The ion trap parameters are taken to be typical for planar traps [11], with ions confined at height $h = 25 \mu\text{m}$ above the plane with an axial frequency ω_i of $2\pi \times 1 \text{ MHz}$. For the commonly used $^9\text{Be}^+$ ion, the harmonic oscillator length is then $z_0 = \sqrt{\hbar/(2m\omega_i)} = 24 \text{ nm}$.

A superconducting inductor is attached to the island electrodes and a silicon bulk-acoustic-wave resonator (BAW) is mounted near the inductor (see the Supplemental Material for technical details). The inductance of 440 nH, combined with the total static circuit capacitance of $C_0 = 46 \text{ fF}$, then yields $\omega_{\text{LC}} = 1 \text{ GHz}$, with characteristic

impedance of $Z = 2.7 \text{ k}\Omega$. The zero-point charge fluctuation on the resonator is $q_0 = \sqrt{\hbar/(2Z)} = 0.9 \text{ electrons}$.

The ion-circuit coupling is provided through two coplanar islands near the ion position that are each connected to a terminal of the superconducting inductor. The microwave electric field between these islands couples to the ion motion along the trap axis through the electric dipole of the moving ion charge. To activate the ion-circuit coupling, one excites acoustic waves in the BAW at frequency $\nu_B \approx \omega_{\text{LC}} - \omega_i$ by voltage driving of metallic electrodes on the BAW surface. The modulation of the BAW-substrate gap distance provides the desired capacitance modulation.

The classical dipole interaction energy of the ion due to the axial electric field E_z from the island electrodes is

$$U_{\text{cl}} = ezE_z = \frac{e\zeta}{h}zV = \frac{e\zeta}{hC}zQ \quad (2)$$

where h is the ion height, V is the voltage between the islands, ζ is a dimensionless constant of order unity set by the electrode geometry, C is the total circuit capacitance, and Q is the total charge on the circuit. Simulation of the electric field near the island electrodes gives $\zeta = 0.25$. The BAW drive modulates the capacitance as $C = C_0(1 + \eta \sin \nu t)$ with modulation depth $\eta = 0.3$, so that

$$U_{\text{cl}}(Q, z, t) = \frac{e\zeta}{hC}(1 - \eta \sin \nu t)zQ \quad (3)$$

We now quantize the LC and ion motion, but keep the BAW motion classical. In the rotating frame with respect to LC and motion, the total Hamiltonian of the ion-LC system becomes (for details of the calculation, see the Supplemental Material)

$$H_{\text{int}}/\hbar = \frac{2ig_0\eta}{3}e^{-i\Delta t}ab^\dagger + \text{h.c.} \quad (4)$$

where $g_0 = e\zeta z_0 q_0/(hC_0)$ and $\Delta \equiv \nu - (\omega_{\text{LC}} - \omega_i)$. For the numerical parameters given above, $g_0 = 2\pi \times 200 \text{ kHz}$ and $\eta = 0.3$, giving $g = 2\pi \times 60 \text{ kHz}$.

Because the BAW is only used as a parametric drive in our scheme, it contributes negligible noise to the LC and motional modes. To first order, the only semiclassical effect of the BAW is variation in the coupling parameter η between the ion motion and the LC—there is no direct (linear) coupling between the motion of the BAW and these other two variables. Hence parametric heating is the main source of noise added by the BAW. While thermal motion of the BAW can in principle produce parametric heating, in most practical settings errors in η will be determined by classical control errors in setting the BAW amplitude.

The chief quantum noise contribution of the BAW arises from the entanglement induced by the LC and ion systems with the BAW and, indirectly, its environment. This entanglement occurs via the parametric coupling,

and manifests as a static displacement of the BAW that depends on LC photon number n_{LC} . The displacement can be estimated as

$$\zeta_{LC} \sim \frac{x_B}{\zeta_0} \frac{n_{LC} \omega_{LC}}{\omega_{LC} - \nu + i\kappa_B/2} \quad (5)$$

where x_B is the harmonic oscillator length of the BAW and κ_B is the BAW damping rate. For typical BAW parameters at $\nu \sim 1$ GHz, one finds $x_B \sim 10^{-16}$ m and $\kappa_B \sim 100$ kHz, so that $\zeta_{LC}/\zeta_0 \lesssim 10^{-3}$ even for $n_{LC} \sim 100$. Hence the BAW contributes negligible quantum noise for our purposes.

LC/spin protocols.—LC/spin protocols can be executed by the swapping method with fidelity well over 95%. Q as high as 5×10^5 have been reported for an LC circuit [12], giving a decoherence rate of 2 ms^{-1} . Motional decoherence rates of 0.5 s^{-1} have been demonstrated in a cryogenically cooled ion trap with an ion height of $150 \mu\text{m}$ and 1 MHz motional frequency [13]. This rate scales as $\sim 1/d^4$ [14], so at our $25 \mu\text{m}$ height, we estimate a rate of 0.5 ms^{-1} . Spin decoherence is negligible on these timescales [7]. Hence the overall decoherence rate is 2.5 ms^{-1} , limited by LC damping. The total spin/LC operation requires two LC/motion swaps, each taking $3 \mu\text{s}$, and the spin/motion protocol, with typical Rabi frequency $\Omega_0 \sim 2\pi \times 100 \text{ kHz}$ [7]. A typical spin/motion protocol requires approximately a $\pi/2$ -pulse time, so the total time required for the LC/spin protocol is $10 \mu\text{s}$. The infidelity is given by the ratio of decoherence rate to operation rate, i.e., 0.03.

Quantum interfaces between LC and spin can be achieved through a Jaynes-Cummings spin/motion interaction [7]. If the LC mode is regarded as the microwave analog of a linear-optical qubit, this interaction serves as a quantum logic interface between ion spin and single-rail microwave photon qubits. A $\pi/2$ pulse of the interaction performs an LC/spin CNOT gate.

An alternative LC-spin quantum interface swaps spin-dependent displacement of the ion motion into the LC mode. The unitary evolution for such a protocol is given by

$$U_{\text{eff}}(\alpha) = \exp[(\alpha a + \alpha^* a^\dagger)\sigma_x] \quad (6)$$

Such an operation could be used to teleport a superposition of spin states into a superposition of coherent LC states.

These interactions allow us to use the LC and ion modes as quantum buses for more complex tasks. The Jaynes-Cummings LC/spin interaction enables quantum communication between LC circuits in independent cryogenic environments, as shown in Figure 3(a). Each ion interface is controllably coupled to a high-finesse optical resonator. After LC/spin coupling, the spin is mapped to the polarisation state of an outgoing optical photon, as in recent experiments [15]. Overall, this set of operations coherently couples the microwave photon

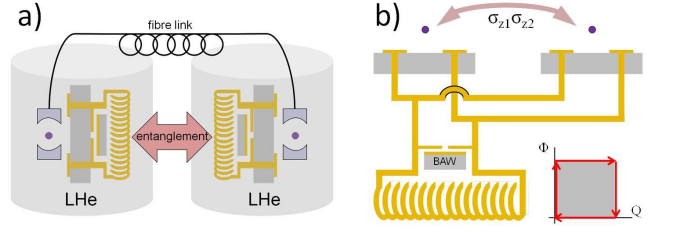


FIG. 3. Quantum buses enabled by LC/motion coupling. a) Quantum communication between LC circuits in independent cryogenic environments. b) Nonlocal ion spin-spin gates on a single chip.

state to the optical domain. In particular, one could entangle independent superconducting qubits via conditional photon measurements [16]. This task is impossible using direct microwave signaling, owing to the thermal noise of microwave links at room temperature.

The spin-dependent LC displacement lets perform nonlocal ion spin-spin gates on a single chip through a shared LC mode (Fig 3(b)). The spin-spin bus is based on the spin-dependent displacement operation $D(\alpha q \sigma_y)$. Two ions (with identical phonon frequencies) in multiple traps are capacitively coupled to the LC circuit. Performing four spin-dependent displacements that enclose a square in phase space with side length $L = \alpha J_z$, one picks up a phase of $2|L|^2 = 4|\alpha|^2(1 + \sigma_z^{(1)}\sigma_z^{(2)})$, which is the desired spin-spin interaction [17]. Along with single qubit gates, this interaction provides a sufficient gate set for universal quantum computation [18].

Spin-dependent displacement of the LC causes a superposition of spin states to evolve into a superposition of LC coherent states. Such superposed coherent states can detect field displacements with Heisenberg-limited sensitivity [19]. In the present context, these states enable Heisenberg-limited metrology of small voltages at microwave frequencies. The mean photon number in the generated state can exceed 100 for our parameters. The RMS voltage is then $\sim 0.1 \text{ mV}$ and can be estimated at sub- μV precision in a single shot.

Resistance to motional heating.—Rapid technical advances in superconducting circuits mean that the LC coherence time may substantially increase in the near future, leaving ion motional heating as the primary source of decoherence. We have developed a modified LC/spin coupling scheme similar to [17, 20] that resists ion heating. We simultaneously apply bichromatic LC/motion and motion/spin couplings at detunings $\pm\delta$ from the blue-sideband and red-sideband resonances. In the frame

rotating with ion motion, the Hamiltonian becomes

$$H_{\text{int}}/\hbar = \sqrt{2}M(x \cos \delta t + p \sin \delta t) \quad (7)$$

$$M \equiv \frac{2i\eta g_0}{3}q + \frac{\Omega_0}{4}\sigma_x \quad (8)$$

where $x = (b+b^\dagger)/\sqrt{2}$, $p = -i(b-b^\dagger)/\sqrt{2}$ are dimensionless motional operators, $q = (a+a^\dagger)/\sqrt{2}$ is the dimensionless charge operator, and we approximate $\Omega_0 \ll \delta \ll \omega_i$. The Hamiltonian (7) is identical to that of [21], except that the collective spin operator J_y is replaced by the collective spin-LC operator M . The ion motional state undergoes M -dependent phase-space displacement along a closed trajectory, giving rise to an M^2 dependent geometric phase. At times $t_n = 2\pi n/|\delta|$ with n an integer, the evolution operator becomes simply

$$U_n = \exp \left[-i \text{sign}(\delta) \frac{2\pi n}{\delta^2} M^2 \right] \quad (9)$$

The undesired q^2 term in Eq. (9) can be removed by a spin echo sequence $ZU_n^\dagger ZU_n$, where $Z = e^{-i\pi\sigma_z}$ is a fast π -pulse of the spin, and U^\dagger is obtained by changing $\delta \rightarrow -\delta$. The overall time evolution is then $\exp(\alpha q\sigma_x)$ with $\alpha = -4i\pi n g_0 \Omega_0 \eta / (3\delta^2)$.

A straightforward modification of the arguments of Sørensen and Mølmer [21] shows that this coupling can be made arbitrarily resistant to ion motional heating. The loss of fidelity due to heating is $\propto 1/\delta^2$ in the limit of low infidelity, while the effective coupling constant is $\propto 1/\delta$. Even if the heating rate is larger than the coupling constant, one can still achieve near-perfect coupling.

Outlook.— Our ion-circuit coupling enables a powerful hybrid quantum system with operation speeds similar to those for ion spins. This system can perform nonlocal quantum gates between ions on a single chip, nonlocal quantum communication between electrical circuits, and Heisenberg-limited voltage metrology. The coupling can be made resistant to ion motional heating. Current experiments in classical ion-circuit coupling [8, 9] can be extended in a natural way to realise our scheme.

This work was supported by the Australian Research Council under DP0773354 (Kielpinski), FF0458313 (Wiseman), the Centre of Excellence for Engineered Quantum Systems and Federation Fellowship funding (Milburn), and by the U.S. Army Research Office MURI award W911NF0910406 and DARPA QUASAR (Taylor). We acknowledge helpful conversations with Timothy Duty.

-
- [1] C. Monroe, *Nature* **416**, 238 (2002).
 - [2] R. Blatt and D. Wineland, *Nature* **453**, 1008 (2008).
 - [3] J. Clarke and F. K. Wilhelm, *Nature* **453**, 1031 (2008).
 - [4] J. Verdú, H. Zoubi, C. Koller, J. Majer, H. Ritsch, and J. Schmiedmayer, *Phys. Rev. Lett.* **103**, 043603 (2009).
 - [5] D. Leibfried, B. DeMarco, V. Meyer, D. Lucas, M. Barrett, J. Britton, W. M. Itano, B. Jelenković, C. Langer, T. Rosenband, and D. J. Wineland, *Nature* **422**, 412 (2003).
 - [6] J. Benhelm, G. Kirchmair, C. F. Roos, and R. Blatt, *Nature Phys.* **4**, 463 (2008), arXiv:0803.2798.
 - [7] D. Leibfried, R. Blatt, C. Monroe, and D. Wineland, *Rev. Mod. Phys.* **75**, 281 (2003).
 - [8] C. Ospelkaus, U. Warring, Y. Colombe, K. R. Brown, J. M. Amini, D. Leibfried, and D. J. Wineland, *Nature* **476**, 181 (2011).
 - [9] N. Timoney, I. Baumgart, M. Johanning, A. F. Varón, M. B. Plenio, A. Retzker, and C. Wunderlich, *Nature* **476**, 185 (2011).
 - [10] J. Chiaverini, R. B. Blakestad, J. Britton, J. D. Jost, C. Langer, D. Leibfried, R. Ozeri, and D. J. Wineland, *Quant. Info. Comp.* **5**, 419 (2005).
 - [11] S. Seidelin, J. Chiaverini, R. Reichle, J. J. Bollinger, D. Leibfried, J. Britton, J. H. Wesenberg, R. B. Blakestad, R. J. Epstein, D. B. Hume, W. M. Itano, J. D. Jost, C. Langer, R. Ozeri, N. Shiga, and D. J. Wineland, *Phys. Rev. Lett.* **96**, 253003 (2006).
 - [12] Z. Kim, C. P. Vlahacos, J. E. Hoffman, J. A. Grover, K. D. Voigt, B. K. Cooper, C. J. Ballard, B. S. Palmer, M. Hafezi, J. M. Taylor, J. R. Anderson, A. J. Dragt, C. J. Lobb, L. A. Orozco, S. L. Rolston, and F. C. Wellstood, *AIP Adv.* **1**, 042107 (2011).
 - [13] J. Labaziewicz, Y. Ge, P. Antohi, D. Leibbrandt, K. R. Brown, and I. L. Chuang, *Phys. Rev. Lett.* **100**, 013001 (2008).
 - [14] Q. A. Turchette *et al.*, *Phys. Rev. A* **61**, 063418 (2000).
 - [15] M. Keller, B. Lange, K. Hayasaka, W. Lange, and H. Walther, *Nature* **431**, 1075 (2004).
 - [16] S. Olmschenk, D. N. Matsukevich, P. Maunz, D. Hayes, L.-M. Duan, and C. Monroe, *Science* **323**, 486 (2009).
 - [17] G. J. Milburn, S. Schneider, and D. F. V. James, *Fortschr. Phys.* **48**, 801 (2000).
 - [18] A. Barenco, C. H. Bennett, R. Cleve, D. P. DiVincenzo, N. Margolus, P. Shor, T. Sleator, J. A. Smolin, and H. Weinfurter, *Phys. Rev. A* **52**, 3457 (1995).
 - [19] W. J. Munro, K. Nemoto, G. J. Milburn, and S. L. Braunstein, *Phys. Rev. A* **66**, 023819 (2002).
 - [20] K. Mølmer and A. Sørensen, *Phys. Rev. Lett.* **82**, 1835 (1999).
 - [21] A. Sørensen and K. Mølmer, *Phys. Rev. A* **62**, 022311 (2000).